Cancer Chemother Pharmacol (2007) 59:537–548
DOI 10.1007/s00280-006-0296-4

ORIGINAL ARTICLE

In vitro and in vivo metabolism of paclitaxel poliglumex: identification of metabolites and active proteases

Scott A. Shaffer · Cassie Baker-Lee · Jacob Kennedy · Man Shun Lai · Peter de Vries · Kent Buhler · Jack W. Singer

Received: 9 April 2006 / Accepted: 17 July 2006 / Published online: 19 August 2006

Abstract
Background The efficacy and tolerability of paclitaxel is limited by its low solubility, high systemic exposure, and a lack of selective tumor uptake. Paclitaxel poliglumex (PPX; XYOTAX™) is a macromolecular drug conjugate that was developed to overcome these limitations; the 2′ hydroxyl group of paclitaxel is linked to a biodegradable polymer, poly-L-glutamic acid, to form an inactive polymeric conjugate. PPX was previously shown to accumulate in tumor tissue, presumably by taking advantage of the hyperpermeable tumor vasculature and suppressed lymphatic clearance in tumor tissue.
Methods Because anti-tumor activity requires the release of paclitaxel from the polymer-drug conjugate, the current report characterizes PPX biodegradation and release of paclitaxel as determined by quantitative HPLC/mass spectral analysis.
Results The identification of monoglutamyl-paclitaxel metabolites in tumor tissue confirmed the in vivo metabolism of PPX in a panel of mouse tumor models. In vitro characterization of the metabolic pathway suggests that PPX can enter tumor cells, and is metabolized to form both mono- and diglutamyl-paclitaxel cleavage products. The intracellular formation of these intermediate metabolites is at least partially dependent on the proteolytic activity of the lysosomal enzyme cathepsin B; PPX metabolism is inhibited by a highly selective inhibitor of cathepsin B, CA-074. Reduced metabolism of PPX in livers and spleens from cathepsin B deficient mice confirms that cathepsin B is an important mediator of PPX metabolism in vivo; however, other proteolytic enzymes may contribute as well.
Conclusions The cathepsin B-mediated release of paclitaxel may have therapeutic implications as cathepsin B is upregulated in malignant cells, particularly during tumor progression.

Keywords Paclitaxel poliglumex · Metabolism · Cathepsin B · Paclitaxel · Intracellular

S. A. Shaffer · C. Baker-Lee · J. Kennedy · M. S. Lai · P. de Vries · K. Buhler · J. W. Singer (✉)
Cell Therapeutics, Inc., 501 Elliott Avenue West, Seattle, WA 98119, USA
e-mail: jsinger@ctiseattle.com

Present Address:
S. A. Shaffer
Department of Medicinal Chemistry, University of Washington, Box 357610, Seattle, WA 98195, USA

Introduction

Paclitaxel, one of the most widely used and clinically active cytotoxic agents, induces mitotic arrest and apoptosis in proliferating cells by targeting tubulin, a component of the mitotic spindle. Paclitaxel binds to the N-terminal 31 amino acids of the β-tubulin subunit and prevents depolymerization. As a result, the mitotic spindle is disabled and cell division cannot be completed [4, 29]. Because the therapeutic index of any cytotoxic agent is related to the length of time that target tissues are exposed to a biologically relevant concentration of active drug [18], low solubility, high systemic exposure, poor pharmacokinetic characteristics, and a lack of selective tumor uptake are all factors limiting the efficacy and tolerability of these agents, including paclitaxel [9, 45, 55]. The rationale for developing paclitaxel poliglumex (PPX), a macromolecular polymer-drug

conjugate, was to improve standard chemotherapy with paclitaxel by overcoming some of these limitations.

Polymer-drug conjugates passively accumulate in tumor tissue because of the enhanced permeability and retention (EPR) effect. Tumor vasculature is more permeable to macromolecules than normal vasculature because of structural differences between the neovasculature in tumors and the mature vasculature in normal organs [13, 42]. The paucity of lymphatic vessels in tumor tissue allows the retention of these macromolecules in the interstitial space, resulting in a 10–100-fold increase in intratumoral drug concentrations when compared with an equivalent dose of the non-conjugated drug [15, 30]. In addition, polymeric conjugation improves the pharmacokinetic profile of cytotoxics by decreasing the volume of distribution and the clearance rate. The prolonged circulation time facilitates tumor accumulation of macromolecules: the EPR effect is optimal for macromolecules with molecular weights of 50–80 kDa, which is well above the renal clearance threshold [8, 33, 47]. The slow release of active drug from the polymer carrier in tumor tissue results in sustained high intratumoral drug levels and lower plasma concentrations of the active drug, potentially reducing treatment-related toxicities. Finally, polymeric conjugation renders hydrophobic agents water-soluble and eliminates the need for toxic solubilizing agents [23].

Paclitaxel poliglumex is a polymer-drug conjugate that links paclitaxel to a biodegradable polymeric backbone consisting of L-glutamic acid residues [48]. Paclitaxel is conjugated by ester linkage to the γ-carboxylic acid side chains of poly-L-glutamic acid, resulting in a relatively stable conjugate. Because the conjugation site is through the 2′ hydroxyl of paclitaxel, a site crucial for tubulin binding, conjugated paclitaxel does not interact with β-tubulin and is biologically inactive [16]. The median molecular weight of PPX is 38.5 kDa; conjugated paclitaxel represents approximately 36%, by weight, of the conjugate, equivalent to about one paclitaxel ester linkage per 11 glutamic acid units of the polymer [49]. PPX accumulates in tumor tissue, and has demonstrated anti-tumor activity in various preclinical tumor models, including ovarian and breast [24–26].

Previously, monoglutamyl-paclitaxel isomers Glu-2′-TXL (2′-[L-γ-glutamyl]-paclitaxel) and Glu-7′-TXL (7′-[L-γ-glutamyl]-paclitaxel) were identified in tumor tissue from B16 tumor bearing mice exposed to [^{3}H]-labeled PPX. Subsequent pharmacokinetic analysis indicated a gradual increase of [^{3}H]-labeled PPX metabolites in tumor tissue, reaching T_{max} at 72 h post-administration. In comparison, administration of [^{3}H]-paclitaxel resulted in a T_{max} at 1.5 h. The gradual accumulation of PPX in tumor tissue was associated with prolonged tumor exposure to PPX metabolites Glu-2′-TXL and paclitaxel. These observations demonstrate the intratumoral degradation of the poliglutamate backbone of PPX in association with the release of paclitaxel [49].

To characterize the pathway by which PPX is degraded to release active drug, its in vivo and in vitro metabolism was evaluated. The kinetics of intracellular formation of several PPX metabolites was quantified in vitro and was found to be largely dependent on the proteolytic activity of the lysosomal enzyme cathepsin B, an exocarboxydipeptidase [54, 56]. This finding may have biological relevance as expression of cathepsin B is upregulated in malignant cells, particularly during tumor progression [37]. These data support a model in which PPX accumulates in tumor tissue through the EPR effect, followed by the cathepsin B-mediated release of paclitaxel.

Results

Assay development

To determine whether PPX could undergo proteolysis to produce the monoglutamyl-paclitaxel isomer Glu-2′-TXL which was previously identified in tumor tissue, PPX was digested with papain, an endopeptidase, in a cell-free system as described in the Data Supplement. Subsequent LC/MS analysis indicated the presence of several peptide–paclitaxel products $(Glu)_n$-TXL ($n = 1$–4), including diglutamyl-paclitaxel isomers (H_2N-Glu-Glu-2′-TXL and HO-Glu-Glu-2′-TXL), monoglutamyl-paclitaxel isomers (Glu-2′-TXL and Glu-7′-TXL), and paclitaxel (TXL).The presence of trace levels of Glu-7′-TXL is not unexpected as PPX has a minor fraction, 2% or less, of paclitaxel conjugated through the paclitaxel -7 position (CTI, data on file).

Identification of these PPX metabolites allowed the development of a quantitative LC/MS assay to analyze PPX biodegradation in vitro and in vivo. Method development is detailed in the Data Supplement.

Quantitation of PPX metabolites in vitro

To characterize the biodegradation of PPX in vitro, murine RAW 264.7 monocyte/macrophage-like cells were used as a model system to study the intracellular metabolism of PPX, as these cells are known to efficiently endocytose molecules with a high molecular weight [39]. RAW 264.7 cells in serum-free media were

exposed to 10 μg/ml PPX. Both cells and media were harvested in duplicate at 0, 0.25, 0.5, 1, 2, 4, 6, 8, 24, 30, 37, and 48 h after continuous PPX exposure. Paclitaxel was the most abundant metabolite in the medium; however, non-enzymatic hydrolysis of paclitaxel from PPX has previously been shown to occur at approximately 12% per 24 h in cell-free conditioned media (data not shown). Because paclitaxel released in the medium is freely diffusible across the cell membrane, mono- and diglutamyl-paclitaxel species, but not paclitaxel, are considered surrogates for the intracellular cleavage of PPX.

The intracellular, time-dependent generation of five PPX metabolites was observed (Fig. 1); paclitaxel, Glu-2′-TXL, and H_2N-Glu-Glu-2′-TXL were most abundant with cellular concentrations peaking at 24–48 h. HO-Glu-Glu-2′-TXL was also observed, but at significantly lower concentrations than the H_2N-Glu-Glu-2′-TXL isomer. HO-Glu-Glu-2′-TXL is relatively unstable as the ester conjugation point is prone to carbonyl attack by the proximate free amine. Notably, no peaks were observed in the ion chromatograms for either $(Glu)_3$-TXL or $(Glu)_4$-TXL molecular species, even though the system was validated to detect these species (Data Supplement).

The in vitro metabolism of PPX was also studied in human HT-29 colon adenocarcinoma and NCI-H460 non-small lung carcinoma cell lines. Although the RAW 264.7 cells tolerated 10 μg/ml PPX, the human carcinoma cell lines were only capable of tolerating 0.6 μg/ml and still remain viable over the course of the experiment. Cell cultures were "pulsed" with PPX 0.6 mg/ml for 4.5 h, and then "chased" with PPX-free media for up to 72 h. This experimental design allowed for the detection of intracellular metabolites from PPX

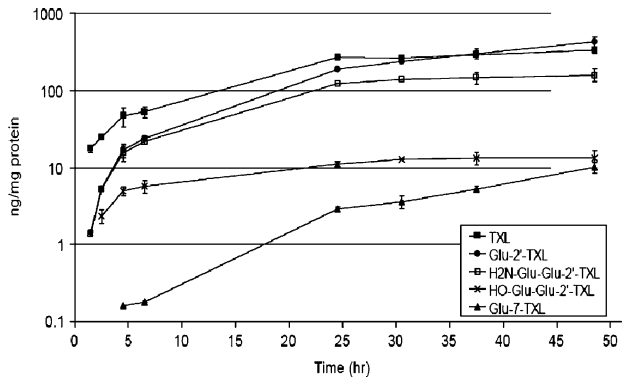

Fig. 1 Profile of PPX metabolites in RAW 264.7 cells as determined by quantitative LC/MS analysis. TXL, Glu-2′-TXL, and H_2N-Glu-Glu-2′-TXL were the most abundant species, with maximum values attained at 24–48 h. HO-Glu-Glu-2′-TXL and Glu-7′-TXL were also observed but at substantially lower levels than their respective isomers

endocytosed during the pulse and eliminated diffusion of free paclitaxel released from PPX by chemical hydrolysis into the cells during the chase. The formation of the five identified PPX metabolites was examined between 0 and 72 h. In NCI-H460 cells, removal of the remaining drug from the media at 4.5 h was followed by the intracellular formation of H_2N-Glu-Glu-2′-TXL, Glu-2′-TXL, and paclitaxel (Fig. 2a). H_2N-Glu-Glu-2′-TXL and Glu-2′-TXL reached maximum concentrations at 24 and 48 h, respectively. A similar pattern was observed in HT-29 cells (Fig. 2b).

Quantitation of PPX metabolites in vitro

To confirm the in vivo biodegradation of PPX in tumor tissue, a panel of seven different tumor models was analyzed by quantitative mass spectrometry. Two syngeneic (B16 and LL/2) and five human colon carcinoma xenografts (HCT-15, LoVo, HT-29, CoLo 320DM, and HCT116) were included; of the latter, HCT-15, LoVo, and Colo 320DM are multi-drug resistant (mdr-1^+). Figure 3 shows the levels of monoglutamyl-TXL PPX metabolites in the different tumor types, indicating that PPX is subject to in vivo proteolysis in all tumor types tested, even in tumor types characterized by highly active drug-efflux pumps [11, 14].

Proteolysis of PPX by cathepsin B

To determine what enzymes are responsible for the metabolism of PPX, an initial panel of commercially available human proteases was screened for proteolytic activity in a cell-free system, including elastase, cathepsin B, cathepsin D, cathepsin G, cathepsin H, cathepsin L, trypsin, chymotrypsin, kallikrein, and gelatinase; the only enzyme able to degrade PPX was cathepsin B (data not shown). The role of cathepsins in the metabolism of PPX was further characterized using a panel of two carboxypeptidases, human liver cathepsin B and mouse recombinant cathepsin X, and two aminopeptidases, bovine spleen cathepsin C and human liver cathepsin H. Incubation of PPX with cathepsin B resulted in predominantly diglutamyl-paclitaxel (i.e., both H_2N-Glu-Glu-2′-TXL and HO-Glu-Glu-2′-TXL); diglutamyl-paclitaxel and monoglutamyl-paclitaxel (i.e., Glu-2′-TXL) were formed at a ~10:1 ratio. Incubation with cathepsin X produced exclusively Glu-2′-TXL (Table 1). This is in agreement with the known specificity of cathepsin X, which functions as an exocarboxymonopeptidase [21]. Aminopeptidases cathepsin C and H were unable to metabolize PPX, presumably because PPX has a N-terminal cyclized pyro-glutamate residue which hinders aminopeptidase

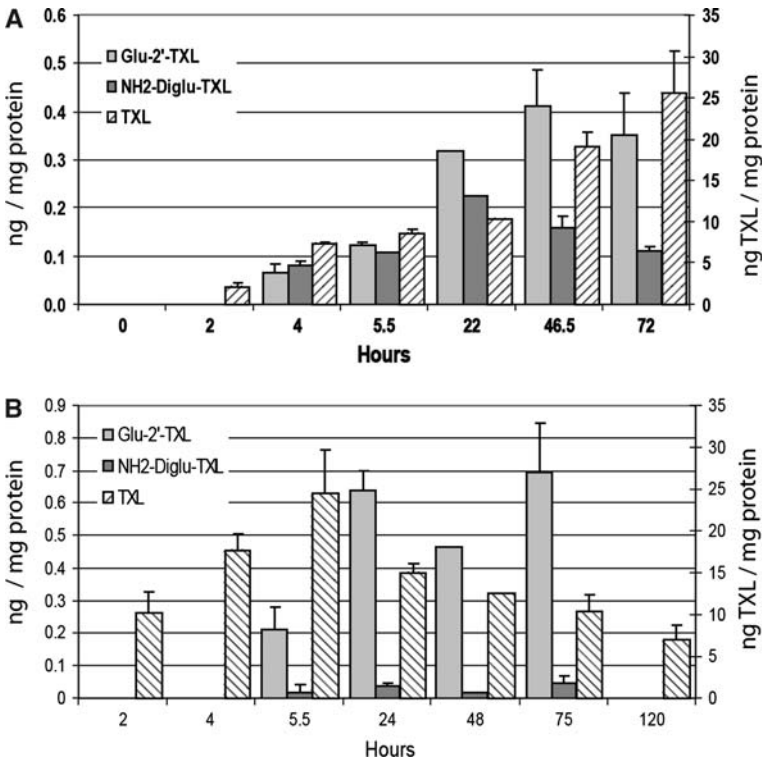

Fig. 2 Paclitaxel poliglumex metabolites in **a** NCI-H460 cells and **b** HT-29 cells. Cells were dosed with PPX for 4.5 h before replacing the medium (pulse/chase). The increased levels of PPX metabolites over time reflect the metabolism of PPX following cellular uptake

activity [2]. However, the combination of cathepsins B, H, and X increased proteolytic activity compared to the combination of cathepsins B, C, and X. Thus, cathepsin H, but not cathepsin C, may contribute to the proteolysis of $(Glu)_n$-TXL fragments containing free amino-termini.

In this cell-free system, the proteolytic activity of cathepsin B was limited as overall reaction rates were <1%. To address this issue, a cathepsin B activity assay measuring cleavage of the synthetic fluorogenic substrate z-Arg-Arg-AMC was used to evaluate the activity of cathepsin B [19]. Cathepsin B was shown to be active for approximately 8–10 min, which provides an explanation for the reproducible, but limited, formation of PPX metabolites in a cell-free environment (data not shown).

In vitro metabolism of PPX by cathepsin B

The biological significance of PPX proteolysis by the lysosomal protease cathepsin B was evaluated in vitro in RAW 264.7 cells using two cell-permeable cysteine

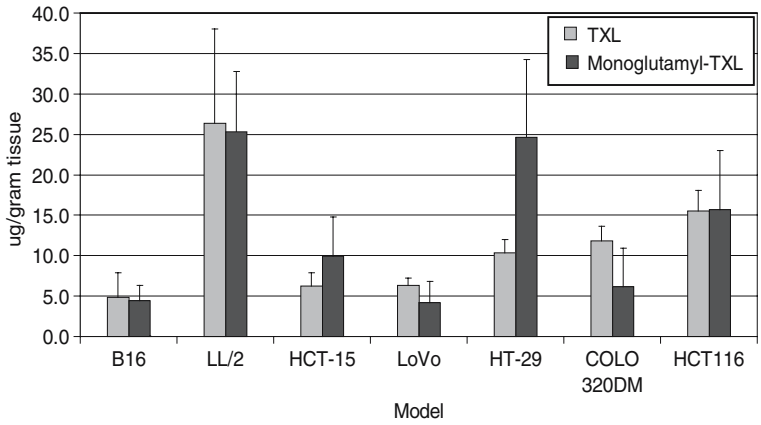

Fig. 3 Paclitaxel poliglumex metabolite concentrations in tumor tissue 24 h post-dosing as determined by quantitative LC/MS analysis. Male nude mice with HCT-15, LoVo, HT-29, CoLo 320 DM, and HCT116 xenografts, as well as female C57BL/6 mice with syngeneic B16 and LL/2 tumors were injected IP at 120 mg/kg TXL equivalents. PPX metabolites are present in tumor tissue from all animal models tested, including those characterized by high drug-efflux pump activity. PPX metabolite levels were higher in MDR− tumor types compared to MDR+ tumor types (*MDR* multi-drug resistant)

Table 1 Reaction products and extent of reaction estimates for PPX incubations with cathepsins B, C, H, and X

	Diglutamyl-TXL (total pmol)	Monoglutamyl-TXL (total pmol)	Total products (pmol)	Extend of reaction (%)
No enzyme	ND	ND	ND	–
Cathepsin B	8.53	0.89	9.4	0.13
Cathepsin C	ND	ND	ND	–
Cathepsin H	ND	ND	ND	–
Cathepsin X	ND	10.5	10.5	0.15
Cathepsin B, C, X	23.6	10.2	33.8	0.48
Cathepsin B, C, H	6.82	0.61	7.43	0.11
Cathepsin B, H, X	53.0	17.0	70.0	1.0
Cathepsin C, H, X		8.45	8.45	0.12
Cathepsin B, C, H, X	57.2	20.8	78.0	1.1

Numbers represent mean values of duplicate measures

ND none detected

protease inhibitors [35]. CA-074 is a highly selective and irreversible inhibitor of cathepsin B; CA-074 has an IC_{50} of ~2.2 nM for cathepsin B, while cathepsin L and H exhibit IC_{50} values of 172 and 420 μM, respectively. EST, or loxistatin, is a general irreversible cysteine protease inhibitor. Both compounds were added to the media at 2 or 5 μM 30 min before PPX dosing at 10 μg/ml. Figure 4 shows the metabolite concentrations at 2, 4, and 6 h. Both inhibitors dramatically inhibited the formation of diglutamyl-TXL and monoglutamyl-TXL isomers, with the maximum effect of >90% inhibition for each of these metabolites at 6 h (EST, 2 μM; CA-074, 5 μM). Cellular levels of mono- and diglutamyl-paclitaxel isomers increased at 23 h post-dosing, reflecting the high turnover rate of the cysteine proteases responsible for PPX metabolism.

In vivo metabolism of PPX by cathepsin B

The availability of a transgenic cathepsin B knock-out mouse model allowed the further characterization of cathepsin B-mediated metabolism of PPX. Because studies in this model with human xenografts or syngeneic tumor cells were not feasible, tissues known to accumulate PPX through endocytosis, such as liver and spleen, were evaluated. First, expected levels of

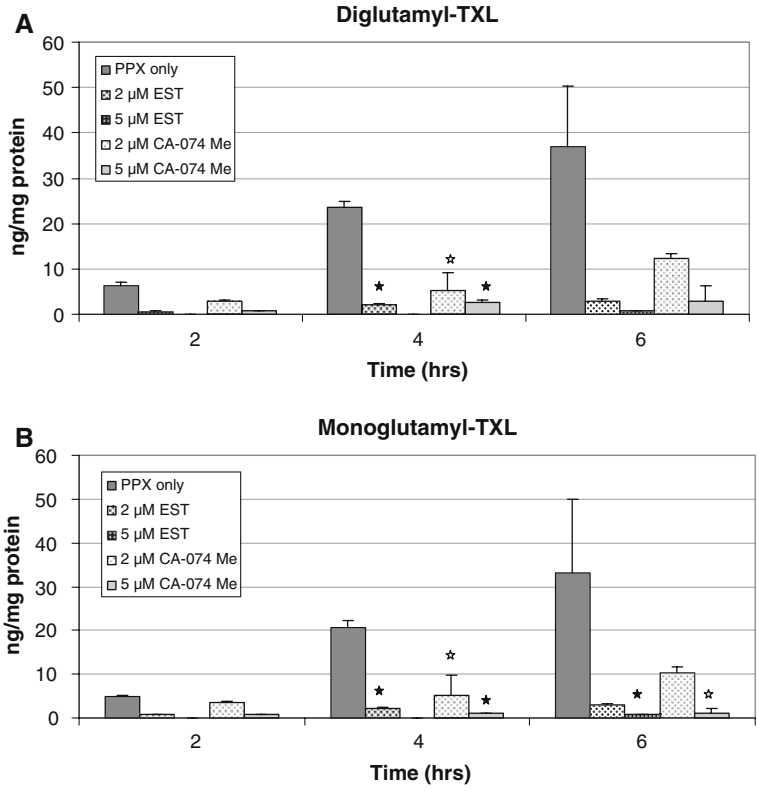

Fig. 4 Cellular levels of diglutamyl-TXL (**a**) and monoglutamyl-TXL (**b**) PPX following exposure to cysteine protease inhibitors. At 4 and 6 h post-dosing, EST (2 μM) and CA-074 Me (5 μM) effectively inhibited PPX metabolism as metabolite levels were decreased ≥90% compared to control (*five-point filled star*, $P < 0.001$; *five-point open star*, $P < 0.05$; Student's *t*-test)

cathepsin B activity were confirmed in liver and spleen homogenates from wild-type (+/+), heterozygote (+/−), and cathepsin B null (-/-) animals by an assay measuring cleavage of z-Arg-Arg-AMC (data not shown; Ref. [28]). Using this assay, no significant cathepsin B activity was observed in plasma from either +/+, +/−, or -/- animals.

Pharmacokinetic parameters were determined using a non-compartmental analysis based on quantitative LC/MS values; results for the different PPX metabolites in liver and spleen homogenates are shown in Fig. 5a and b. The metabolism of PPX in cathepsin B -/- animals was reduced compared to heterozygote and wild-type animals: (1) the T_{max} values for diglutamyl-paclitaxel isomers were delayed; (2) C_{max} values were reduced for both di- and monoglutamyl-paclitaxel isomers; and (3) AUC values were reduced for all PPX metabolites (Table 2). These data suggest that cathepsin B is an important in vivo mediator of PPX metabolism and the subsequent release of paclitaxel; however, other proteolytic pathways contribute, or compensate, as well.

No relevant PPX metabolites other than paclitaxel were detected in the plasma compartment of these non-tumor bearing animals. Interestingly, while in males plasma pharmacokinetic parameters were consistent between phenotypes, the plasma paclitaxel AUC was reduced by 70% in mutant females compared to normal females (Fig. 5c). This observation,

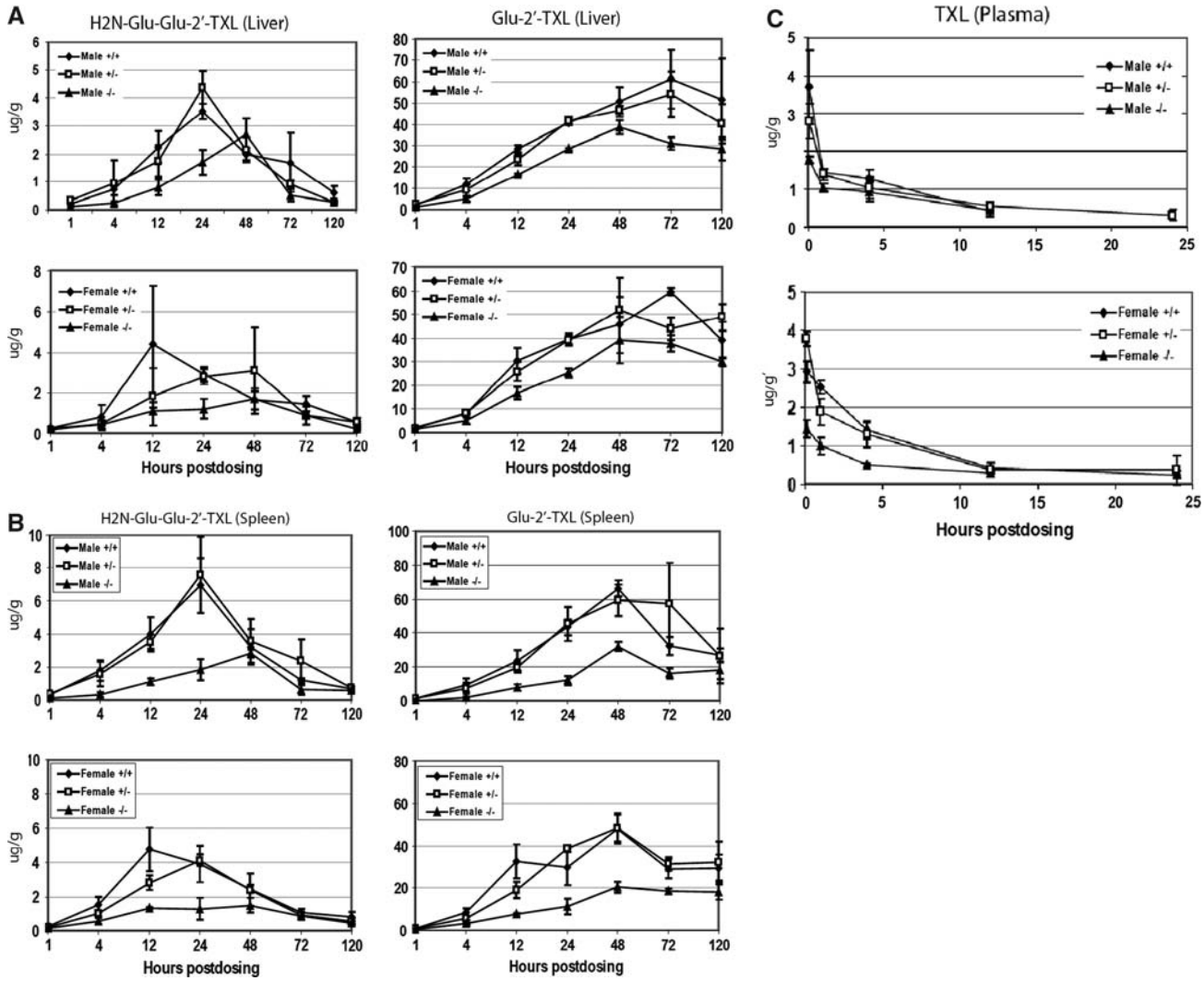

Fig. 5 In vivo PPX metabolism in transgenic cathepsin B mice; (+/+) represents wild-type; (−/−) represents knock-out; (+/−) represents heterozygous. Profile shown for H_2N-Glu-Glu-2′-TXL is representative for changes over time observed for OH-Glu-Glu-2′-TXL (not shown). **a** Levels of PPX metabolites in the liver of male and female mice after administration of PPX. **b** Levels of PPX metabolites in the spleen of male and female mice after administration of PPX. **c** Levels of paclitaxel over time in the plasma of male and female mice after administration of PPX. Animals were dosed with 80 mg/kg PPX as a single tail vein injection of approximately 0.25 ml (10 ml/kg) of a 25-mg/ml solution in saline

Table 2 Paclitaxel poliglumex metabolites in liver and spleen homogenates from a transgenic cathepsin B knock-out mouse model: % changes in pharmacokinetic parameters between wild-type and cathepsin B-deficient animals

Genotype	Variable	H_2N-Glu-Glu-2′-TXL	Glu-2′-TXL	TXL
Liver				
Female (+/+)	T_{max} (h)	12	72	0.083
	C_{max} (μg/g)	4.4	59.6	12.9
	AUC	206	5,249	884
Female (+/−)	T_{max} (h)	48	48	0.083
	C_{max} (μg/g)	3.1	51.8	13.3
	AUC	192	5,006	719
	ΔAUC (% from wt)	*−7.2*	*−4.6*	*−18.6*
Female (-/-)	T_{max} (h)	48	48	0.083
	C_{max} (μg/g)	1.7	39.1	8.0
	AUC	112	3,678	495
	ΔAUC (% from wt)	*−45.7*	*−29.9*	*−44.0*
Male (+/+)	T_{max} (h)	24	72	1.0
	C_{max} (μg/g)	3.5	61.2	11.6
	AUC	213	5,740	973
Male (+/−)	T_{max} (h)	24	72	0.083
	C_{max} (μg/g)	4.4	54.0	14.1
	AUC	194	5,062	999
	ΔAUC (% from wt)	*−8.9*	*−11.8*	*2.6*
Male (-/-)	T_{max} (h)	48	48	0.083
	C_{max} (μg/g)	2.7	38.4	13.6
	AUC	131	3,424	686
	ΔAUC (% from wt)	*−38.5*	*−40.3*	*−29.5*
Spleen				
Female (+/+)	T_{max} (h)	12.0	48.0	120.0
	C_{max} (μg/g)	4.8	47.7	6.3
	AUC	244	3,811	5.3
Female (+/−)	T_{max} (h)	24	48	120
	C_{max} (μg/g)	4.1	48.3	4.0
	AUC	213	3,975	411
	ΔAUC (% from wt)	*−12.7*	*4.3*	*−18.3*
Female (-/-)	T_{max} (h)	48	48	72
	C_{max} (μg/g)	1.5	20.3	3.8
	AUC	118	1,884	360
	ΔAUC (% from wt)	*−51.7*	*−50.6*	*−28.4*
Male (+/+)	T_{max} (h)	24	48	48
	C_{max} (μg/g)	7.0	66.3	5.9
	AUC	306	4,257	509
Male (+/−)	T_{max} (h)	24	48	72
	C_{max} (μg/g)	7.6	59.3	5.6
	AUC	364	5,183	530
	ΔAUC (% from wt)	*18.4*	*21.8*	*4.2*
Male (-/-)	T_{max} (h)	48	48	48
	C_{max} (μg/g)	2.8	32.0	2.4
	AUC	150	2,085	213
	ΔAUC (% from wt)	*−50.9*	*−51.0*	*−58.2*

together with dramatic shift in liver T_{max} values for the diglutamyl-paclitaxel isomers noted in mutant females, suggests that cathepsin B-mediated PPX metabolism may differ between males and females.

Discussion

The lack of tumor specificity and relatively poor pharmacokinetic characteristics of small, hydrophobic cytotoxic agents has led to the design of macromolecular drug conjugates that link these agents to biocompatible, water-soluble polymers [15]. The high molecular weight of the resulting new chemical entity changes the pharmacological characteristics of the cytotoxic agent by prolonging circulation time and facilitating tumor accumulation through the EPR effect [9]. Macromolecules with a molecular weight of more than 40 kDa cannot be internalized into cells by simple diffusion; instead, macromolecules have been shown to enter cells through endocytosis, which is particularly efficient during mitosis [10, 34, 36]. Next, the active component is released

from the polymeric backbone by the proteolytic activity of lysosomal enzymes, followed by diffusion of the active agent into the cytoplasm or nucleus [8].

Paclitaxel poliglumex has been shown to accumulate in tumor tissue in a mouse tumor model [24]. Pharmacokinetic studies have shown that PPX is relatively stable in plasma; in preclinical studies, unconjugated paclitaxel represented less than 1% of total paclitaxel in plasma [49]. The current study provides evidence for the intratumoral degradation of PPX, as was suggested by the identification of both monoglutamyl-paclitaxel isomers, Glu-2′-TXL and Glu-7-TXL, in seven different tumor types. The further analysis and quantitation of PPX metabolites in an in vitro system verified the biodegradation of PPX through the formation of diglutamyl-paclitaxel and monoglutamyl-paclitaxel metabolites, as well as paclitaxel. In NCI-H460 cells, removal of the drug by replacing the media at 4.5 h post-exposure was followed by the formation of H_2N-Glu-Glu-2′-TXL, Glu-2′-TXL, and TXL; H_2N-Glu-Glu-2′-TXL and Glu-2′-TXL reached maximum concentrations at 24 and 48 h, respectively. More importantly, however, paclitaxel concentrations continued to increase over the time course, confirming the intracellular release of paclitaxel. These observations indicate that PPX can enter tumor cells, presumably through endocytosis [8]. Following endocytosis, macromolecules are contained within endosomal/lysosomal vesicles as demonstrated by the enhanced release of the conjugated compound finding through the incorporation of lysosomally degradable spacers [20]. The specific proteolysis of PPX by cathepsin B, a lysosomal enzyme, is consistent with the intracellular metabolism of PPX following endocytosis.

Cathepsin B is a papain-family cysteine protease that is normally located in lysosomes, where it is involved in the turnover of proteins and plays various roles in maintaining the normal metabolism of cells. Under normal physiological conditions, cathepsin B expression and activity is tightly regulated [59]. In malignant tumors and premalignant lesions, however, increased cathepsin B mRNA expression is associated with elevated cathepsin B protein levels and activity, and correlates with tumor invasion in glioma [41, 51], colorectal carcinoma [5, 17, 31], and prostate carcinoma [50]. Cathepsin B precursors are normally targeted to the endosomal/lysosomal compartment via the mannose-6-phosphate receptor pathway [28]. The intracellular trafficking of cathepsin B is often altered in malignant tumors, resulting in the increased secretion of precursor and active forms of the enzyme [1, 27, 38, 40], its redistribution from perinuclear lysosomes to peripheral vesicles [52], and its association with the cell membrane [46, 52, 53]. Cathepsin B localizes with other proteases at the tumor cell surface in caveolae, mediating cell-surface proteolytic events associated with invasion [6, 44]. The abundance of cathepsin B in tumor tissue is relevant for the efficient degradation of PPX. While in vivo studies show that PPX is clearly metabolized intratumorally, further in vivo studies are required to confirm that PPX is metabolized intracellularly following endocytosis, or within the interstitial tumor space through pericellular cathepsin B activity, or perhaps both.

Paclitaxel poliglumex metabolism is not completely dependent on cathepsin B, as was shown in the transgenic cathepsin B mouse model. Redundancy between the activities of cathepsins may exist; however, the in vitro data indicate that only the carboxy exopeptidases, cathepsin B and X, could mediate PPX metabolism. Cathepsin B produces predominantly diglutamyl-paclitaxel through carboxydipeptidase activity while cathepsin X produces monoglutamyl-paclitaxel through carboxymonopeptidase activity [54]. While it is unclear whether the subsequent release of paclitaxel occurs through hydrolysis or requires additional enzymatic cleavage, the specific inhibition of cathepsin B activity was clearly associated with reduced release of paclitaxel. Unlike cathepsin B, expression of cathepsin X is limited to cells of the immune system, and its protein levels are low in two malignant cell lines that highly expressed cathepsin B [21]. Interestingly, prostatic intraepithelial neoplasias and prostate carcinomas were found to have upregulated levels of cathepsin X in association with low levels of cathepsin B [32]. The extent of cathepsin X-mediated metabolism of PPX, particularly in prostate cancer, as well as cathepsin-independent degradation of PPX requires further investigation.

The formation of diglutamyl-paclitaxel isomers occurred at a different rate in female mice compared to males; T_{max} values were reached at 12 h vs. 24 h, respectively. However, in the cathepsin B -/- animals, T_{max} values were reached at 48 h, regardless of gender. This observation implies that cathepsin B-mediated degradation of PPX may be more important in females. In support of this suggestion, the levels of free paclitaxel in plasma are significantly reduced in the mutant females compared to heterozygotes or normal females; in contrast, paclitaxel plasma levels are similar in cathepsin B -/-, +/−, and +/+ males. The hormonal regulation of proteases has been described [12, 43], and estrogen is a well-known modulator of cathepsin activity [3, 22, 57, 58]. The interactions between estrogen, estrogen receptors, and cathepsin B activity may affect PPX metabolism depending on tissue or tumor characteristics, and are currently under investigation.

In summary, PPX is a macromolecular polymer-drug conjugate that links paclitaxel to poly-L-glutamic acid.

PPX is stable in plasma, and accumulates in tumors by taking advantage of the EPR effect. Anti-tumor activity is dependent upon the release of paclitaxel from the polymeric backbone. The current study demonstrates the enzymatic degradation of PPX in vivo: PPX metabolites, diglutamyl- and monoglutamyl-paclitaxel, as well as paclitaxel, were identified in several tumor models. In vitro assays showed that the release of conjugated paclitaxel was dependent on the activity of cathepsin B, a lysosomal enzyme that is over-expressed in many tumor types. Data from a cathepsin B deficient animal model confirmed that cathepsin B is an important in vivo mediator of PPX metabolism and the subsequent release of paclitaxel; however, other proteolytic pathways contribute as well.

Materials and methods

In vitro studies

Cell-free enzymatic proteolysis of PPX

The proteolytic activity of cathepsin was characterized using Cathepsins B (human liver, Calbiochem), C (bovine spleen, Sigma), H (human liver, Calbiochem, San Diego, CA, USA), and X (recombinant mouse, R&D Systems Inc., Minneapolis, MN, USA) with substrate/enzyme ratios of 20:1. PPX (1 mg/ml), cathepsin C (0.1 mg/ml), cathepsin B (0.1 mg/ml), and cathepsin H (0.1 mg/ml) were prepared in reaction buffer [20 mM sodium acetate, 2 mM EDTA (pH 5.0), 5 mM dithiothreitol]. Cathepsin X (0.1 mg/ml) was prepared in activation buffer [25 mM sodium acetate (pH 3.0) and 5 mM dithiothreitol], and was kept at room temperature for 5 min for activation prior to incubation. For incubation, 16 μl PPX and 8 μl enzyme were added to 184 μl reaction buffer; all incubations were carried out for 30 min at 37°C.

Cell-based enzymatic proteolysis of PPX

RAW 264.7 cells (ATTC TIB-71) were grown in RPMI 1640 with 2% fetal bovine serum (FBS). NCI-H460 (ATCC HTB-177) human non-small lung carcinoma cells were grown in RPMI 1640 + 2 mM L-glutamine supplemented with 1.5 g/l sodium bicarbonate, 4.5 g/l glucose, 10 mM HEPES (pH 7.2–7.5), 1 mM sodium pyruvate, and 10% (v/v) heat-treated FBS. HT-29 human colon adenocarcinoma cells (ATCC HTB-38) were grown in McCoy's 5A medium (modified) supplemented with 1 mM sodium pyruvate, 2 mM L-glutamine, 100,000 U/l penicillin, 100,000 μg/l streptomycin, and 10% (v/v) heat-treated FBS.

Cells were plated in 10 cm plates and grown to ~50% confluence. Immediately prior to dosing, the growth medium was removed from each plate and replaced with serum-free medium. PPX was added at a final concentration of 0.6–10 μg/ml in PBS. PPX and control cultures were harvested in duplicate at various time points between 0 and 72 h. For harvest, the medium was transferred to a silanized glass tube and any suspended cells or cell debris was removed by centrifugation; supernatants were stored at −70°C. The plates were rinsed twice with 5 ml chilled PBS and the cells were scraped into an additional 5 ml of PBS before separating with gentle pipetting. A 4.5 ml aliquot of the resultant cell suspension was then pelleted for LC/MS analysis. The remaining ~0.5 ml aliquot was used for total protein determination using a BCA (Pierce Biotechnology Inc., Rockford, IL, USA) assay.

For treatment with protease inhibitors, RAW 264.7 cells were grown as described. On the day of dosing the medium was removed and replaced with 10 ml of RPMI just prior to the addition of either CA-074 Me (BIOMOL Research Laboratories Inc.) or EST (Calbiochem). Inhibitors were added as single doses at 2 or 5 μM 30 min before PPX dosing, and were delivered in DMSO. Plates that did not receive either inhibitor were dosed with the corresponding DMSO vehicle. At 2, 4, and 6.4 h after dosing with PPX (10 μg/ml), duplicate plates were harvested as described before. Controls were harvested at 0 and 23 h. Cells and media were stored at −70°C prior to analysis. Total protein was determined as described.

Sample preparation for HPLC/mass spectrometry (LC/MS)

Each cell pellet or medium sample was acidified with 1% (v/v) acetic acid. Samples were spiked with 100 ng of both d_5-TXL and H_2N-Glu-Glu-2′-d_5-TXL just prior to extraction. Cell pellets and medium (i.e., either 200 μl or 1.0 ml) were extracted with ethyl acetate [1% (v/v) acetic acid], followed by centrifugation at ~750*g* for 10 min for phase separation. The organic phase was transferred and evaporated to ~30 μl under N_2 at room temperature. The sample was then brought to a volume of ~300 μl with a 1:1 mixture of H_2O/CH_3CN (1:1) and 1% acetic acid, and transferred to a 300 μl crimp top LC vial for quantitative LC/MS analysis.

In vivo studies

Tumor models

Male nude mice [Taconic Farms, Hudson, NY, USA Tac:Cr:(NCr)-Foxn-1(nu) male], aged 6–7 weeks at

time of arrival, were used for all experiments with HCT-15, LoVo, HT-29, CoLo 320 DM, and HCT116 tumors. Female C57BL/6 mice (Taconic Farms) were used for the B16 and LL/2 tumors. B16, LL/2, HCT-15, LoVo, HT-29, CoLo 320DM, and HCT116 cell lines were obtained from the ATCC. Mice were injected with tumor cells subcutaneously and allowed to reach a specified tumor volume, <100 mm^3 in most cases, prior to dosing with PPX. PPX was prepared in 0.1 N Na_2HPO_4 at a concentration of 13 mg/ml for dosing. All mice were injected IP at 120 mg/kg TXL equivalents. Mice were euthanized by cervical dislocation. Tumors were harvested and stored at −70°C until further analysis.

Transgenic cathepsin B knock-out mouse model

Two breeding pairs of cathepsin B (+/−) heterozygotes were supplied by Dr Thomas Reinheckel, University of Freiburg (Freiburg, Germany) through the laboratory of Dr Richard Meyers, Stanford University (Stanford, CA, USA) [7]. Subsequent interbreeding of the heterozygous animals produced offspring of all three genotypes: wild-type (+/+), heterozygous (+/−), and knock-out (-/-). Animals received the equivalent of 80 mg/kg free paclitaxel using a PPX solution of 25 mg/ml in saline (32% TXL loading) as a single tail vein injection. At each harvesting time point, plasma and tissues from triplicate animals were anesthetized and plasma and tissues were collected as described above. The time points of tissue collection were at 5 min and 1, 4, 12, 24, 48, 72, and 120 h post-dose. Plasma, liver, and spleen samples were collected on ice, immediately transferred to −70°C, and stored prior to processing.

Sample preparation for LC/MS

For HPLC/MS analysis, tissues were thawed on an ice bath and homogenized using a tissue tearor in 4 ml PBS. The homogenate was then transferred to a 50-ml glass tube and the internal standard, 1.0 μg of d_5-paclitaxel (CTI, lot 1120-02), was added as 100 μl of a 10 μl/ml stock solution prepared in MeOH. For extraction, 15 ml of EtOAc was added and the tubes vortexed thoroughly and placed on ice. Samples were then centrifuged for 2 × 10 min at 900*g* in a swinging-bucket rotor centrifuge to promote phase separation. The upper organic phase was carefully transferred to a new glass tube and stored at −70°C. Extracts were evaporated to near dryness under N_2 in a water bath at ~50°C. Periodically, the sides of the tube were rinsed with EtOAc as the evaporation progressed. The sample was then brought to a volume of ~300 μl with a 1:1 mixture of H_2O/CH_3CN (1:1) and 1% acetic acid, and transferred to a 300-μl crimp top LC vial for quantitative LC/MS analysis.

Analytical methods

LC/MS

Samples were analyzed using a Shimadzu (Columbia, MD, USA) VP HPLC system using a Taxsil-3 column (5 μ, 2.0 mm × 150 mm; MetaChem Technologies, Torrance, CA, USA) and guard column (MetaChem). Mass spectrometry was performed on an electrospray ionization triple quadrupole mass spectrometer (Waters, Manchester, UK) fitted with an electrospray orthogonal "Z" spray ion interface operating in the positive ion mode. Methods and validation of the quantitative LC/MS assay are detailed in the Data Supplement.

Acknowledgments The authors wish to recognize the following individuals for outstanding technical and intellectual contributions: Martha Anderson, Brian Baker, Garland Bellamy, Rama Bhatt, Lynn Bonham, Scott Burke, Jessica Freiberg, Allison Harmon, Anil Kumar, Ruthanne Naranjo, Ed Nudelman, Clint Reigh, Ivan Stone, and Jennifer Thompson. The authors thank Dr Thomas Reinheckel (University of Freiburg) and Dr Richard Meyers (Stanford University) for providing the transgenic cathepsin B mice.

References

1. Achkar C, Gong QM, Frankfater A, Bajkowski AS (1990) Differences in targeting and secretion of cathepsins B and L by BALB/3T3 fibroblasts and Moloney murine sarcoma virus-transformed BALB/3T3 fibroblasts. J Biol Chem 265:13650–13654
2. Awade AC, Cleuziat P, Gonzales T, Robert-Baudouy J (1994) Pyrrolidone carboxyl peptidase (Pcp): an enzyme that removes pyroglutamic acid (pGlu) from pGlu-peptides and pGlu-proteins. Proteins 20:34–51
3. Balan KV, Hollis VW, Eckberg WR, Ayorinde F, Karkera JD, Wyche JH, Anderson WA (2001) Cathepsin B and complement C3 are major comigrants in the estrogen-induced peroxidase fraction of rat uterine fluid. J Submicrosc Cytol Pathol 33:221–230
4. Bhalla KN (2003) Microtubule-targeted anticancer agents and apoptosis. Oncogene 22:9075–9086
5. Campo E, Munoz J, Miquel R, Palacin A, Cardesa A, Sloane BF, Emmert-Buck MR (1994) Cathepsin B expression in colorectal carcinomas correlates with tumor progression and shortened patient survival. Am J Pathol 145:301–309
6. Cavallo-Medved D, Mai J, Dosescu J, Sameni M, Sloane BF (2005) Caveolin-1 mediates the expression and localization of cathepsin B, pro-urokinase plasminogen activator and their cell-surface receptors in human colorectal carcinoma cells. J Cell Sci 118:1493–1503
7. Deussing J, Tisljar K, Papazoglou A, Peters C (2000) Mouse cathepsin F: cDNA cloning, genomic organization and chromosomal assignment of the gene. Gene 251:165–173

8. Duncan R (2003) The dawning era of polymer therapeutics. Nat Rev Drug Discov 2:347–360
9. Duncan R, Spreafico F (1994) Polymer conjugates. Pharmacokinetic considerations for design and development. Clin Pharmacokinet 27:290–306
10. Duncan R, Rejmanova P, Kopecek J, Lloyd JB (1981) Pinocytic uptake and intracellular degradation of N-(2-hydroxypropyl)methacrylamide copolymers. A potential drug delivery system. Biochim Biophys Acta 678:143–150
11. Fojo AT, Ueda K, Slamon DJ, Poplack DG, Gottesman MM, Pastan I (1987) Expression of a multidrug-resistance gene in human tumors and tissues. Proc Natl Acad Sci USA 84:265–269
12. Gallagher LJ, Sloane BF (1984) Effect of estrogen on lysosomal enzyme activities in rat heart. Proc Soc Exp Biol Med 177:428–433
13. Gerlowski LE, Jain RK (1986) Microvascular permeability of normal and neoplastic tissues. Microvasc Res 31:288–305
14. Goldstein LJ, Galski H, Fojo A, Willingham M, Lai SL, Gazdar A, Pirker R, Green A, Crist W, Brodeur GM et al (1989) Expression of a multidrug resistance gene in human cancers. J Natl Cancer Inst 81:116–124
15. Greish K, Fang J, Inutsuka T, Nagamitsu A, Maeda H (2003) Macromolecular therapeutics: advantages and prospects with special emphasis on solid tumour targeting. Clin Pharmacokinet 42:1089–1105
16. Gueritte-Voegelein F, Guenard D, Lavelle F, Le Goff MT, Mangatal L, Potier P (1991) Relationships between the structure of taxol analogues and their antimitotic activity. J Med Chem 34:992–998
17. Hirai K, Yokoyama M, Asano G, Tanaka S (1999) Expression of cathepsin B and cystatin C in human colorectal cancer. Hum Pathol 30:680–686
18. Horton JK, Houghton PJ, Houghton JA (1988) Relationships between tumor responsiveness, vincristine pharmacokinetics and arrest of mitosis in human tumor xenografts. Biochem Pharmacol 37:3995–4000
19. Hulkower KI, Butler CC, Linebaugh BE, Klaus JL, Keppler D, Giranda VL, Sloane BF (2000) Fluorescent microplate assay for cancer cell-associated cathepsin B. Eur J Biochem 267:4165–4170
20. Jensen KD, Nori A, Tijerina M, Kopeckova P, Kopecek J (2003) Cytoplasmic delivery and nuclear targeting of synthetic macromolecules. J Control Release 87:89–105
21. Kos J, Sekirnik A, Premzl A, Zavasnik Bergant V, Langerholc T, Turk B, Werle B, Golouh R, Repnik U, Jeras M, Turk V (2005) Carboxypeptidases cathepsins X and B display distinct protein profile in human cells and tissues. Exp Cell Res 306:103–113
22. Kremer M, Judd J, Rifkin B, Auszmann J, Oursler MJ (1995) Estrogen modulation of osteoclast lysosomal enzyme secretion. J Cell Biochem 57:271–279
23. Li C (2002) Poly(L-glutamic acid)—anticancer drug conjugates. Adv Drug Deliv Rev 54:695–713
24. Li C, Yu DF, Newman RA, Cabral F, Stephens LC, Hunter N, Milas L, Wallace S (1998) Complete regression of well-established tumors using a novel water-soluble poly(L-glutamic acid)-paclitaxel conjugate. Cancer Res 58:2404–2419
25. Li C, Price JE, Milas L, Hunter NR, Ke S, Yu DF, Charnsangavej C, Wallace S (1999) Antitumor activity of poly(L-glutamic acid)-paclitaxel on syngeneic and xenografted tumors. Clin Cancer Res 5:891–897
26. Li C, Newman RA, Wu QP, Ke S, Chen W, Hutto T, Kan Z, Brannan MD, Charnsangavej C, Wallace S (2000) Biodistribution of paclitaxel and poly(L-glutamic acid)-paclitaxel conjugate in mice with ovarian OCa-1 tumor. Cancer Chemother Pharmacol 46:416–422
27. Linebaugh BE, Sameni M, Day NA, Sloane BF, Keppler D (1999) Exocytosis of active cathepsin B enzyme activity at pH 7.0, inhibition and molecular mass. Eur J Biochem 264:100–109
28. Lorenzo K, Ton P, Clark JL, Coulibaly S, Mach L (2000) Invasive properties of murine squamous carcinoma cells: secretion of matrix-degrading cathepsins is attributable to a deficiency in the mannose 6-phosphate/insulin-like growth factor II receptor. Cancer Res 60:4070–4076
29. Manfredi JJ, Parness J, Horwitz SB (1982) Taxol binds to cellular microtubules. J Cell Biol 94:688–696
30. Matsumura Y, Maeda H (1986) A new concept for macromolecular therapeutics in cancer chemotherapy: mechanism of tumoritropic accumulation of proteins and the antitumor agent smancs. Cancer Res 46:6387–6392
31. Murnane MJ, Sheahan K, Ozdemirli M, Shuja S (1991) Stage-specific increases in cathepsin B messenger RNA content in human colorectal carcinoma. Cancer Res 51:1137–1142
32. Nagler DK, Kruger S, Kellner A, Ziomek E, Menard R, Buhtz P, Krams M, Roessner A, Kellner U (2004) Up-regulation of cathepsin X in prostate cancer and prostatic intraepithelial neoplasia. Prostate 60:109–119
33. Noguchi Y, Wu J, Duncan R, Strohalm J, Ulbrich K, Akaike T, Maeda H (1998) Early phase tumor accumulation of macromolecules: a great difference in clearance rate between tumor and normal tissues. Jpn J Cancer Res 89:307–314
34. Oda T, Maeda H (1987) Binding to and internalization by cultured cells of neocarzinostatin and enhancement of its actions by conjugation with lipophilic styrene-maleic acid copolymer. Cancer Res 47:3206–3211
35. Otto HH, Schirmeister T (1997) Cysteine proteases and their inhibitors. Chem Rev 97:133–172
36. Pellegrin P, Fernandez A, Lamb NJ, Bennes R (2002) Macromolecular uptake is a spontaneous event during mitosis in cultured fibroblasts: implications for vector-dependent plasmid transfection. Mol Biol Cell 13:570–578
37. Podgorski I, Sloane BF (2003) Cathepsin B and its role(s) in cancer progression. Biochem Soc Symp 70:263–276
38. Poole AR, Tiltman KJ, Recklies AD, Stoker TA (1978) Differences in secretion of the proteinase cathepsin B at the edges of human breast carcinomas and fibroadenomas. Nature 273:545–547
39. Raschke WC, Baird S, Ralph P, Nakoinz I (1978) Functional macrophage cell lines transformed by Abelson leukemia virus. Cell 15:261–267
40. Recklies AD, Poole AR, Mort JS (1982) A cysteine proteinase secreted from human breast tumours is immunologically related to cathepsin B. Biochem J 207:633–636
41. Rempel SA, Rosenblum ML, Mikkelsen T, Yan PS, Ellis KD, Golembieski WA, Sameni M, Rozhin J, Ziegler G, Sloane BF (1994) Cathepsin B expression and localization in glioma progression and invasion. Cancer Res 54:6027–6031
42. Roberts WG, Palade GE (1997) Neovasculature induced by vascular endothelial growth factor is fenestrated. Cancer Res 57:765–772
43. Rochefort H, Capony F, Augereau P, Cavailles V, Garcia M, Morisset M, Freiss G, Maudelonde T, Vignon F (1987) The estrogen-regulated 52K-cathepsin-D in breast cancer: from biology to clinical applications. Int J Rad Appl Instrum B 14:377–384
44. Roshy S, Sloane BF, Moin K (2003) Pericellular cathepsin B and malignant progression. Cancer Metastasis Rev 22:271–286

45. Rowinsky EK, Donehower RC (1995) Paclitaxel (taxol). N Engl J Med 332:1004–1014
46. Sameni M, Elliott E, Ziegler G, Fortgens PH, Dennison C, Sloane BF (1995) Cathepsin B and D are localized at the surface of human breast cancer cells. Pathol Oncol Res 1:43–53
47. Seymour LW, Miyamoto Y, Maeda H, Brereton M, Strohalm J, Ulbrich K, Duncan R (1995) Influence of molecular weight on passive tumour accumulation of a soluble macromolecular drug carrier. Eur J Cancer 31A:766–770
48. Singer JW, Baker B, De Vries P, Kumar A, Shaffer S, Vawter E, Bolton M, Garzone P (2003) Poly-(L)-glutamic acid-paclitaxel (CT-2103) [XYOTAX], a biodegradable polymeric drug conjugate: characterization, preclinical pharmacology, and preliminary clinical data. Adv Exp Med Biol 519:81–99
49. Singer JW, Shaffer S, Baker B, Bernareggi A, Stromatt S, Nienstedt D, Besman M (2005) Paclitaxel poliglumex (XYOTAX; CT-2103): an intracellularly targeted taxane. Anticancer Drugs 16:243–254
50. Sinha AA, Quast BJ, Korkowski JC, Wilson MJ, Reddy PK, Ewing SL, Sloane BF, Gleason DF (1999) The relationship of cathepsin B and stefin A mRNA localization identifies a potentially aggressive variant of human prostate cancer within a Gleason histologic score. Anticancer Res 19:2821–2829
51. Sivaparvathi M, Sawaya R, Wang SW, Rayford A, Yamamoto M, Liotta LA, Nicolson GL, Rao JS (1995) Overexpression and localization of cathepsin B during the progression of human gliomas. Clin Exp Metastasis 13:49–56
52. Sloane BF, Moin K, Sameni M, Tait LR, Rozhin J, Ziegler G (1994) Membrane association of cathepsin B can be induced by transfection of human breast epithelial cells with c-Ha-ras oncogene. J Cell Sci 107(Pt 2):373–384
53. Spiess E, Bruning A, Gack S, Ulbricht B, Spring H, Trefz G, Ebert W (1994) Cathepsin B activity in human lung tumor cell lines: ultrastructural localization, pH sensitivity, and inhibitor status at the cellular level. J Histochem Cytochem 42:917–929
54. Therrien C, Lachance P, Sulea T, Purisima EO, Qi H, Ziomek E, Alvarez-Hernandez A, Roush WR, Menard R (2001) Cathepsins X and B can be differentiated through their respective mono- and dipeptidyl carboxypeptidase activities. Biochemistry 40:2702–2711
55. ten Tije AJ, Verweij J, Loos WJ, Sparreboom A (2003) Pharmacological effects of formulation vehicles: implications for cancer chemotherapy. Clin Pharmacokinet 42:665–685
56. Turk V, Turk B, Turk D (2001) Lysosomal cysteine proteases: facts and opportunities. EMBO J 20:4629–4633
57. Waters KM, Safe S, Gaido KW (2001) Differential gene expression in response to methoxychlor and estradiol through ERalpha, ERbeta, and AR in reproductive tissues of female mice. Toxicol Sci 63:47–56
58. Westley BR, May FE (1987) Oestrogen regulates cathepsin D mRNA levels in oestrogen responsive human breast cancer cells. Nucleic Acids Res 15:3773–3786
59. Yan S, Sloane BF (2003) Molecular regulation of human cathepsin B: implication in pathologies. Biol Chem 384:845–854